

# Verification of skin-based markers for 3-dimensional kinematic analysis of the equine tarsal joint

S. KHUMSAP\*, J. L. LANOVAZ† and H. M. CLAYTON‡

\*Faculty of Veterinary Medicine, Chiang Mai University, Thailand; †Department of Mechanical and Material Engineering, Queen's University, Kingston, Ontario, Canada; and ‡McPhail Equine Performance Center, Michigan State University, East Lansing, Michigan, USA.

**Keywords:** horse; hock; kinematic; 3-dimensional; trot

## Summary

**Reasons for performing study:** Kinematic studies are usually based on tracking markers attached to the skin. However, complex joints, such as the tarsal joint, function in 3-dimensions (3D), and have therefore necessitated application of the invasive bone pin technique, limiting kinematic studies to the research laboratory. This study investigates the feasibility of using skin-based markers for 3D analysis of tarsal joint motion.

**Hypothesis:** Three-dimensional motions of the tarsal joint can be measured with an acceptable degree of accuracy using skin markers.

**Methods:** Retroreflective markers were attached over the tibial and metatarsal segments. Markers were tracked automatically at trot. Three-dimensional skin correction algorithms were used for correction of skin displacement, and 3D motions derived from the corrected (CSD) and uncorrected (USD) skin displacement were compared with data from a previous study in which those motions were described using bone-fixed markers (BFM) by correlation, root mean square errors (RMS) and shape agreement (SA) of the curves.

**Results:** The RMS of BFM and CSD were smaller than those of BFM and USD for all motions. The correlation coefficients of BFM and CSD were higher than those of BFM and USD. SA was good or fair for all motions except internal/external rotation and medial/lateral translation.

**Conclusions and potential relevance:** With appropriate correction for skin movement relative to skeletal landmarks, skin markers can identify tarsal 3D motions for flexion/extension, abduction/adduction, cranial/caudal translation, and proximal/distal translation, allowing analysis and comparison of information between horses during swing and stance phases.

## Introduction

The application of gait analysis as a clinical tool requires the use of accurate, noninvasive methods of data collection. Movements of the equine limb joints distal to the shoulder and hip are primarily those of flexion and extension and, consequently, published kinematic studies have focused on 2-dimensional analysis in the

sagittal plane. However, complex joints, such as the tarsal joint, may not function as simple hinges. Three-dimensional (3D) motions of the equine tarsal joint complex have been described by tracking the movements of marker triads fixed to the tibia and metatarsus (Lanovaz *et al.* 2002a). Measurable amounts of tarsal joint motion were found in the frontal (abduction and adduction) and transverse (axial rotation) planes, some of which occurred outside the tarsocrural joint. The invasiveness of the bone pin technique limits its application to the research laboratory. In the clinical gait laboratory, kinematic studies are usually based on tracking markers attached to the skin. Verification of the accuracy of skin markers for measuring motion of the tarsal joint complex outside the sagittal plane is an important step towards using this technique in the evaluation of performance and lameness.

The objective of this study was to verify the feasibility of using skin-based markers to evaluate 3D movements of the tarsal joint. The hypothesis was that 3D rotational and translational motions of the equine tarsal joint complex can be measured with an acceptable degree of accuracy using skin markers.

## Materials and methods

Four sound horses were selected on the basis of physical evaluation, combined with radiography and nuclear scintigraphy of the tarsal joints (Khumsap *et al.* 2003). Six Falcon infrared video cameras (Motion Analysis System)<sup>1</sup> collected data at 120 frames/sec. Twelve retroreflective skin-based markers, which could be viewed from the lateral side, were attached to the skin over anatomical landmarks of the tibial and metatarsal segments of the right hindlimb, as described by Lanovaz *et al.* (2004). Two additional reference markers were attached on the medial malleolus of the tibia and the dorsal edge of the head of the second metatarsal bone (MtII). The horse was positioned obliquely to the longitudinal axis of the data collection volume so all the markers could be seen by at least 2 cameras. A video recording, named the reference pose, was captured and the 2 reference markers on the medial side of the limb were then removed. The handler led the horse at trot through the data collection volume. To ensure that all horses moved at an equivalent speed, data collection was performed as described in Khumsap *et al.* (2003) until at least 5 successful trials had been obtained from each horse. Mean  $\pm$  s.d. speed for the 4 horses was  $2.87 \pm 0.05$  m/sec.

\*Author to whom correspondence should be addressed.

[Paper received for publication 10.05.04; Accepted 25.10.04]

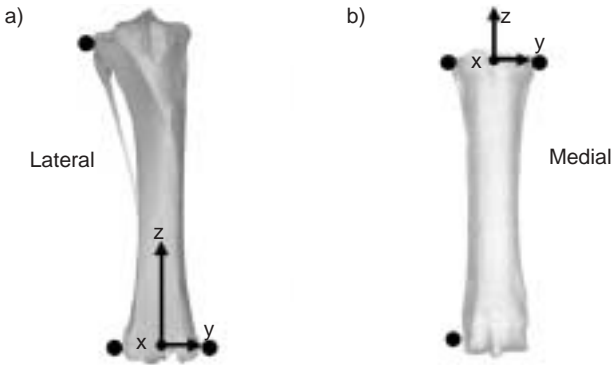


Fig 1: Cranial views of a) the right tibia and b) the right metatarsal bone showing positions of retroreflective markers (●) used to establish the segmental coordinate systems. Origins of the coordinate systems were located midway between the distal tibial markers and midway between the proximal third metatarsal markers. The positive directions were medial for the flexion/extension axis (y), craniodorsal for the abduction/adduction axis (x) and proximal for the internal/external rotation axis (z).

The tibial segmental coordinate system (SCS) was constructed from the markers at the distal attachment of the lateral collateral ligament of the femorotibial joint, lateral malleolus and medial malleolus (Fig 1). The first axis to be defined was the flexion/extension axis (y), which was a vector running from lateral malleolus to medial malleolus. This vector was positive in a lateral to medial direction. The second axis was the abduction/adduction axis (x), which was calculated as a vector perpendicular to both the y-axis and a line from the lateral malleolus to the proximal tibial marker. This axis was positive in a caudal to cranial direction. The third axis was the internal/external rotation axis (z), which was calculated as a vector perpendicular to both x- and y-axes that was positive in a distal to proximal direction. The origin of the tibial SCS was embedded in the bone midway between lateral and medial malleoli.

The metatarsal SCS was constructed using markers over the dorsal edges of the heads of the fourth and second metatarsals, and the lateral condyle on the distal McIII (Fig 1). The flexion/extension (y) axis was a vector from McIV to the McII, which was positive in a lateral to medial direction. The abduction/adduction (x) axis was perpendicular to the y-axis and to a line from the head of McIV to the distal condyle of the McIII. The y-axis was positive in a plantar to dorsal direction. The internal/external rotation (z) axis was mutually perpendicular to x- and y-axes, and was positive in a distal to proximal direction. The origin of the metatarsal SCS was embedded in the bone midway between the dorsal edges of the heads of McIV and McII.

The reference pose was used to relate the location of the skin markers overlying each segment to its SCS. During the trotting trials, skin markers were tracked and expressed in terms of the global coordinate system (GCS). A singular-value decomposition method (Söderkvist and Wedin 1993) was used to transform the skin marker locations from the GCS to their corresponding SCS for each frame during the stride. Skin marker corrections were applied using mean skin displacement values (Lanovaz *et al.* 2002b) to restore the tibial and metatarsal SCSs.

Complete 3D kinematic analysis of the tarsal joint complex involved the measurement of relative rotational and translational motions between the tibial and metatarsal SCSs. In this study, all motions were measured as movement of the metatarsus relative to

TABLE 1: Pearson correlation coefficients (r) and root mean square (RMS) errors between bone-fixed marker data (BF) from Lanovaz *et al.* (2002) and data corrected (C) or uncorrected (U) for skin displacement in the tarsal joint. Correlation coefficients shown are statistically significant ( $P < 0.05$ ). Nonsignificant correlation coefficients are shown as NSD. Shape agreement (SA) was evaluated qualitatively for similarity in shape and magnitude between BF and C curves

Motion	r		RMS errors		SA
	BF vs. C	BF vs. U	BF vs. C	BF vs. U	BF vs. C
<b>Stance</b>					
Flexion/extension	0.93	0.92	$2.38 \pm 0.82$	$3.05 \pm 1.24$	Good
Abduction/adduction	0.53	0.21	$1.19 \pm 1.02$	$1.45 \pm 0.67$	Fair
Internal/external rot	NSD	NSD	$2.29 \pm 0.10$	$8.62 \pm 0.81$	Poor
Cranial/caudal trans	0.82	0.43	$5.06 \pm 2.10$	$5.89 \pm 1.65$	Fair
Medial/lateral trans	0.37	0.22	$1.83 \pm 0.37$	$4.36 \pm 0.96$	Poor
Proximal/distal trans	0.6	0.76	$2.51 \pm 0.32$	$6.18 \pm 0.57$	Fair
<b>Swing</b>					
Flexion/extension	0.99	0.98	$2.83 \pm 0.82$	$3.55 \pm 1.67$	Good
Abduction/adduction	0.88	-0.12	$1.63 \pm 0.70$	$5.93 \pm 0.61$	Good
Internal/external rot	NSD	NSD	$2.73 \pm 1.49$	$9.35 \pm 1.35$	Poor
Cranial/caudal trans	0.93	0.83	$6.56 \pm 3.26$	$10.58 \pm 2.96$	Good
Medial/lateral trans	NSD	0.29	$2.89 \pm 1.59$	$7.54 \pm 2.97$	Poor
Proximal/distal trans	0.91	0.94	$5.19 \pm 2.84$	$12.29 \pm 4.52$	Fair

trans = translation; rot = rotation.

the fixed tibia, expressed in terms of spatial attitude vectors (Woltring 1994). There were 3 relative rotational motions between the 2 segments: flexion/extension, abduction/adduction and internal/external rotation. Flexion/extension was motion around the y-axis; negative values were assigned for flexion, and positive values were assigned for extension. Abduction/adduction was motion around the x-axis; negative values were assigned for abduction and positive values for adduction. Internal/external rotation was motion around the z-axis; negative values were assigned for external rotation and positive values for internal rotation. Translational motions were measured in 3 directions; cranial/caudal, medial/lateral and proximal/distal translations. Cranial/caudal translation was motion along the x-axis; negative values were assigned for caudal translation and positive values for cranial translation. Medial/lateral translation was motion along the y-axis; negative values were assigned for lateral and positive values for medial translation. Proximal/distal translation was motion along the z-axis; negative values were assigned for distal and positive values for proximal translation.

Rotational and translational motions, both before and after the application of skin correction algorithms, were obtained separately for stance and swing phases, and expressed relative to the values at the start of the stance phase of that stride. Data derived from 5 strides were combined and a mean curve for each horse was constructed to represent that horse's movement pattern. The true rotational and translational motions of the tarsal joint, derived from bone-fixed markers data (BFD) (Lanovaz *et al.* 2002a) from the same group of horses, were used as reference values. The mean curves for the 3D motions from the corrected (CSD) and uncorrected (USD) skin displacement data of each horse were compared with the true motions of the tarsal joint. Root mean square (RMS) errors were calculated for each horse, and the mean RMS errors for the group were then calculated. Pearson product moment correlation was used to compare BFD and CDS or USD at a significance level of  $P < 0.05$ . To explore similarities and differences in the shape of the curves, the true motion of the joint was plotted together with uncorrected and

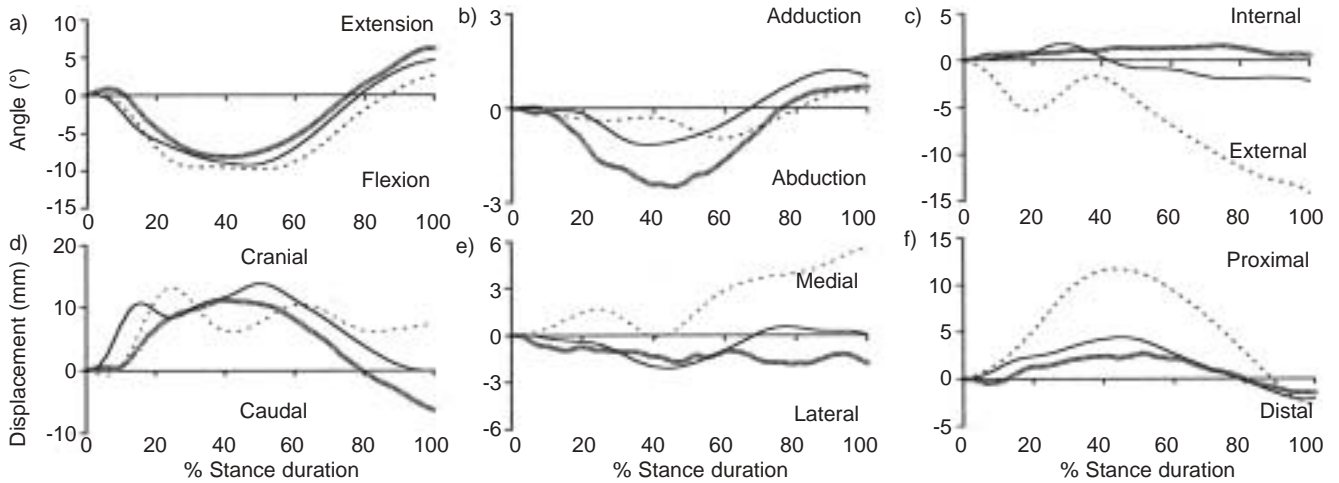


Fig 2: Mean curves of 3D rotational and translational motions of the tarsal joints during stance: a) extension(+)/flexion(-) angle; b) adduction(+)/abduction(-) angle; c) internal(+)/external(-) rotation angle; d) cranial(+)/caudal(-) translation; e) medial(+)/lateral(-) translation; and f) proximal(+)/distal(-) translation. Solid line = corrected skin data; dashed line = uncorrected skin data; dotted line = bone-fixed marker data from Lanovaz *et al.* (2002). Zero indicates the impact value.

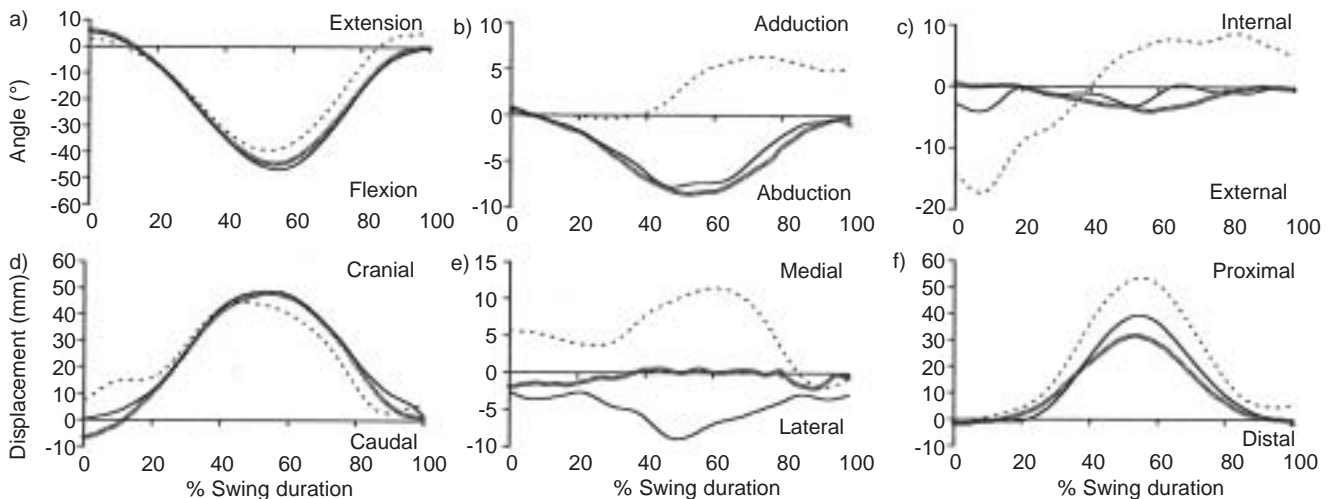


Fig 3: Mean curves of 3D rotational and translational motions of the tarsal joints during swing. For details see Figure 2.

corrected skin data. Agreement between BFD and CSD curves was evaluated qualitatively and assessed as 'good' when the shape and direction of the curves were similar for the 2 sets of data; 'fair' when the curves showed minor differences in direction or magnitude; and 'poor' when neither the shape nor direction of the curves were similar.

## Results

The RMS errors of BFD and CSD were smaller than those of BFD and USD for all motions (Table 1). The correlation coefficients of BFD and CSD were higher than those of BFD and USD for cranial/caudal translation, flexion/extension and abduction/adduction ( $P < 0.05$ ) during stance and swing phases. Visual comparison of the curves for CSD and USD with the curve for BFD (Figs 2 and 3) shows a much closer agreement following correction for skin displacement, especially for abduction/adduction in swing. In general, shape agreement between BFD and CSD was better during swing than during stance. Stance phase data indicated good shape agreement between BFD and CSD for flexion/extension

and fair shape agreement for abduction/adduction, cranial/caudal translation and proximal/distal translation. During the swing phase (Fig 3), there was good shape agreement between the curves representing BFD and CSD for flexion/extension, abduction/adduction and cranial/caudal translation and fair shape agreement for proximal/distal translation. These results support acceptance of the experimental hypothesis for all motions except internal/external rotation and medial/lateral translation.

## Discussion

The tarsal joint complex consists of 4 joints. The major motion is flexion/extension at the tarsocrural joint. The motions at the other 3 joints, proximal intertarsal, distal intertarsal and tarsometatarsal joints, are considered to be small. Due to the oblique orientation of the talar ridges, flexion/extension of the tarsocrural joint is accompanied by translational motion, which is characteristic of helical motion (Badoux 1987). The largest force loading the distal tibia is a torsional force (Schneider *et al.* 1982; Hartman *et al.* 1984). The combination of torsional loading from the tibia and the

oblique orientation of the talus may lead to motion at the other 3 low-motion joints in the tarsal joint complex. The objective of this study was to develop a noninvasive method of measuring 3D motion of the tarsal joint complex. Since the segments between the 3 distal tarsal joints are extremely short it is not possible to attach skin markers to represent each segment of the tarsal joint complex, although some assumptions could be made regarding the motion of these joints. The tarsocrural joint has a screw motion (Badoux 1987; Lanovaz *et al.* 2002a), which implies that rotational and translational motions of the tarsocrural joint in any direction are highly coupled with flexion/extension of this joint. Loss of coupling between flexion/extension and the other motions suggests movement at tarsal joints outside the tarsocrural joint (Lanovaz *et al.* 2002a).

The use of correction algorithms for skin displacement is important for obtaining accurate kinematic data from skin-based markers. In order to study 3D kinematics of the tarsal joints using skin-based markers, it was necessary to develop 3D skin correction algorithms based on knowledge of the motion of the underlying bones. The advantage of this study was that the data were obtained from the same horses that had been used to construct skin correction algorithms in a previous study (Lanovaz *et al.* 2002a,b, 2004). By using the same horses for both studies, it enhanced the ability to test how closely the skin correction algorithms could correct skin marker data to real bone motion in an individual horse.

Data from bone-fixed markers indicated that there was some variation among horses in rotational and translational motions, as shown by the relatively wide s.d. for abduction/adduction and proximal/distal translation. Therefore, the skin correction algorithms, which were calculated as the best fit for a group of horses, might not be able to account for individual variation in all motions. Nevertheless, the comparison between BFD and CSD showed higher correlation coefficients and smaller RMS errors than the comparison between BFD and USD, indicating that the application of skin correction algorithms enhances the quality of motions derived from skin-based markers. Improvements in the shape of the curves following correction for skin displacement are clearly visible in Figures 2 and 3.

During stance, shape agreement between BFD and CSD was assessed as good for flexion/extension, fair for 3 other degrees of freedom, and poor for the other 2 degrees of freedom. Even though the RMS errors for internal/external rotation and medial/lateral translation between BFD and CSD were small, there was no statistically significant correlation between those motions. In addition, shape agreement between BFD and CSD of those motions was poor. Therefore, it is not suggested that this 3D skin-marker set be used for testing changes in these 2 motions. For abduction/adduction and proximal/distal translation, the directions of motion were correct, but differences in the magnitude of the movement resulted in the shape agreement being assessed as fair. For cranial/caudal displacement, the fair assessment was due to differences in shapes of the curves in early stance, whereas in midstance the curves were quite similar. Therefore, comparisons between conditions for these ranges of motion within an individual horse should be acceptable, but direct comparisons between different horses should be avoided due to the possibility of under- or overestimation of joint motion from skin-based data.

The curves showed better shape agreement during swing than during stance. During swing, assessment of shape agreement was good for 3 motions, fair for one motion and poor for 2 motions. Internal/external rotation and medial/lateral translation showed poor shape agreement for the same reasons as described during stance. Therefore, it is not suggested that this 3D skin marker set be used to obtain information describing these 2 motions during swing. Proximal/distal translation showed fair agreement in shape, mainly due to overestimation of proximal displacement in mid swing, although the value still fell within 1 s.d. of the real bone motion from Lanovaz *et al.* (2002a). Therefore, swing phase flexion/extension, abduction/adduction, cranial/caudal translation and proximal/distal translation ranges of motion can be estimated with acceptable accuracy from corrected skin data. The relatively good 3D information obtained from this skin marker set during swing allows analysis and comparison of information between horses.

From this study, it is concluded that, with appropriate correction for skin displacement, skin-based markers can identify tarsal 3D motions with acceptable accuracy for flexion/extension, abduction/adduction, cranial/caudal translation and proximal/distal translation, but not for internal/external rotation or medial/lateral translation.

### Acknowledgements

This study was funded by the McPhail Endowment and the Department of Large Animal Clinical Sciences, Michigan State University.

### Manufacturer's address

<sup>1</sup>Motion Analysis Corporation, Santa Rosa, California, USA.

### References

- Badoux, D. (1987) Some biomechanical aspects of the structure of the equine tarsus. *Anatom. Anzeiger*. **164**, 53-61.
- Hartman, W., Schamhardt, H., Lammertink, J. and Badoux, D. (1984) Bone strain in the equine tibia: an *in vivo* strain gauge analysis. *Am. J. vet. Res.* **45**, 880-884.
- Khumsap, S., Lanovaz, J.L., Rosenstein, D.L., Byron, C. and Clayton, H.M. (2003) Effect of unilateral synovitis of distal intertarsal and tarsometatarsal joints on sagittal plane kinematics and kinetics of trotting horses. *Am. J. vet. Res.* **64**, 1491-1495.
- Lanovaz, J.L., Khumsap, S. and Clayton, H.M. (2004) Quantification of 3D skin displacement artifacts on the equine tibia and third metatarsus. *Equine comp. exerc. Physiol.* **1**, 141-150.
- Lanovaz, J.L., Khumsap, S., Clayton, H.M., Stick, J.A. and Brown, J. (2002a) Three-dimensional kinematics of the tarsal joint at the trot. *Equine vet. J., Suppl.* **34**, 308-313.
- Lanovaz, J.L., Khumsap, S., Clayton, H.M. (2002b) The development of corrections for skin displacement artefacts at the equine tarsal joint and application to 3D joint kinematics. In: *Biomechanics of the Equine Tarsal Joint*. PhD Thesis, Ed: S. Khumsap, Michigan State University, East Lansing. pp 204-233.
- Schneider, R., Milne, D., Gabel, A., Groom, J. and Bramlage, L. (1982) Multidirectional *in vivo* strain analysis of the equine radius and tibia during dynamic loading with and without a cast. *Am. J. vet. Res.* **43**, 1541-1550.
- Söderkvist, I. and Wedin, P. (1993) Determining the movements of the skeleton using well-configured markers. *J. Biomech.* **26**, 1473-1477.
- Woltring, H.J. (1994) 3D attitude representation of human joints: a standardization proposal. *J. Biomech.* **27**, 1399-1414.